Düzce Üniversitesi Bilim ve Teknoloji Dergisi

Araştırma Makalesi

Synthesis of Metal (Ni) Doped Metal Oxide (ZnO) Heteronanostructures and Investigation of Their Morphological-Optical Properties

Mustafa BİÇER

[a] *Department of Chemistry, Faculty of Arts and Sciences, Düzce University, TURKİYE*
** Sorumlu yazarın e-posta adresi: mustafabicer@duzce.edu.tr*
DOI: 10.29130/dubited.1167452

ABSTRACT

In this study, different volumes of Nickel (Ni) doped Zinc oxide (ZnO) thin films were deposited on FTO by hydrothermal method. The films were characterized by SEM, EDS, and UV-Vis Spectroscopy. When the SEM images were examined, the nanostructures showed different morphological features as the amount of doped (v) nickel-ZnO increased in comparison to undoped nickel-ZnO. Furthermore, it was demonstrated that the obtained film surface has a homogeneous distribution. EDS spectra showed the increase in Ni by volume and its presence in the film composition. The UV-Vis Spectroscopy results showed that Ni doping can change the transmittance and band gap values from 2.94 to 3.38, and thus the ZnO band gap can be adjusted by Ni doping. As a result of the findings, ZnO-NiO thin films are promising candidates for both high-performance hetero nanostructures and practical applications.

Keywords: *Nanostructures, ZnO-NiO thin films, Hydrothermal method, Band gap*

Metal (Ni) Katkılı Metal Oksit (ZnO) Heteronanoyapıların Sentezi ve Morfolojik-Optik Özelliklerinin İncelenmesi

Öz

Bu çalışmada, hidrotermal yöntemle FTO üzerine farklı hacimlerde Nikel (Ni) katkılı Çinko oksit (ZnO) ince filmler biriktirilmiştir. Filmler SEM, EDS ve UV-Vis Spektroskopisi ile karakterize edildi. SEM görüntüleri incelendiğinde katkılı (v) nikel-ZnO miktarı katkısız nikel-ZnO'ya göre arttığı için nanoyapılar farklı morfolojik özellikler göstermiştir. Ayrıca elde edilen film yüzeyinin homojen bir dağılıma sahip olduğu gösterildi. EDS spektrumları, Ni'nin hacimce katılımı ve film bileşimindeki varlığı ile Ni miktarının arttığını tespit edilmiştir. UV-Vis Spektroskopisi sonuçları, Ni katkılamanın geçirgenlik ve bant aralığı değerlerini 2,94'ten 3,38'e değiştirebileceğini ve böylece ZnO bant boşluğunun Ni katkılaması ile ayarlanabileceğini göstermiştir. Elde edilen bulgular sonucunda ZnO-NiO ince filmler hem yüksek performanslı hetero nanoyapılar hem de pratik uygulamalar için umut verici adaylardır.

Anahtar Kelimeler: *Nanoyapılar, ZnO-NiO ince filmler, Hidrotermal metot. Bant aralığı*

Geliş: 26/08/2022, Düzeltme: 10/09/2022, Kabul: 20/12/2022

I. INTRODUCTION

Metal oxide nanoparticles play a very important role in many fields of physics, materials and engineering science, especially chemistry. Metal elements can form a plenty variety of oxide compounds. Metal oxide semiconductor devices are more reliable due to their various features such as high temperature operation, chemical stability, thermal stability, low cost, easy manufacturing, long life [1]. In technological applications, metal oxide semiconductor nanoparticles are used for corrosion passivation of surfaces used in manufacturing in solar cells, sensors, microelectronic circuits, fuel cells, piezoelectric devices, coatings and catalysts. Metal oxides such as ZnO, TiO_2, NiO, CuO are often used for the mentioned applications [2], [3].

As one of the metal oxide nanoparticles, zinc oxide (ZnO) plays an important role as a vital semiconductor with enormous technological and scientific interest. In addition, ZnO contains an enormous list of attractive features. ZnO is defined as a strategic, functional, versatile and encouraging inorganic material with a wide range of applications. It is classified as an II-VI semiconductor [4] because Zn and O are identified two and six in the periodic table and in groups, respectively. ZnO has specific semiconducting, optical, chemical sensing, electrical conductivity, and piezoelectric characteristics [5]. It has a elavated excitonic binding energy at room temperature and a direct broad bandgap in the near UV spectrum [6], [7]. Moreover, it is characterized by its inherent n-type electrical conductibility [8]. Because of these properties, ZnO has a wide range of applications [9]. ZnO thin films are considered a possible material for working in the ultraviolet spectral regions and visible in optoelectronic applications due to their distinguishing optical and electrical properties [10]. ZnO thin films are extensively used in various industrial fields such as solar cells [11], [12], UV light emitting devices [13], [14], photocatalysts [15], [16], and ethanol gas sensors [17], [18].

Nickel oxide (NiO), another metal oxide nanoparticle, has a wide direct band gap of ~3.6–4.0 eV at room temperature, high hole mobility, as well as p-type semitakenctor materials [19]. Moreover, it is attracting much attention due to its attractive properties such as low lattice mismatch with ZnO. NiO emerges as an significant transition metal oxide materials with cubic lattice structure used in many implementations [20], [21]. Nanostructured NiO thin films have a extensive range of applications, such as magnetic materials, fuel cells, battery electrodes, photo-electron devices, dye-sensitive photocathodes, ion storage materials, gas sensors, thermoelectric materials, catalysts, electrochromic films, cytotoxic activity, anticancer properties and non-enzymatic glucose sensors etc. [22], [23]. Furthermore, because nano-sized particles differ from most nanoparticles in a number of properties such as unique optical, surface area/volume ratio, electro-optical, magneto-optical, electronic-physicochemical, and chemical-mechanical properties, NiO thin films are investigated [24]. With developments in all fields of industry and technology, attention has been drawn to nanoscale materials resulting from the preference for new properties in their size and morphology, this scale of length, and equally important these properties [25].

In particular, nanostructured ZnO and NiO thin films are encouraging materials for various applications such as biosensors, light-emitting diodes, solar cells, ultraviolet (UV) photodetectors, gas and chemical sensors, and other sensor devices. In the light of these explanations; while ZnO nanostructures have property to exhibit piezoelectric and n-type semiconductor properties [26], NiO nanostructures exhibit non-piezoelectric properties and can have p-type semiconductor properties [27]. The heteronano structure properties of engineered metal oxide nanoparticles can greatly assist in selectivity delimitation. Nanostructured ZnO and NiO thin films are well-known semiconductor materials with nanostructure properties that are being developed to improve heteronanostructure properties [28], [29]. The heterojunction interface is composed by a metal oxide semiconductor nanoparticles from n-type ZnO and p-type NiO, and functions as the p-n junction. Among these heteronanostructures, especially ZnO-NiO hybrids have attracted great attention. As a p-type semiconductor, NiO is useful for the constitution of p-n heterojunctions with ZnO. Therefore, it has features such as high hole mobility, high hole concentration and low lattice mismatch with ZnO thin films. The nano-sized heteronanostructures of ionic metal oxides have drawn much interest as they have developed physico-chemical properties

compared to their one-component counterparts. Quite a few p-n heteronanostructures have been reported, employing the properties of both nanostructured NiO thin films and nanostructured ZnO thin films in combination. There are few explores on the production of p-type NiO and n-type ZnO heteronanostructures with different techniques in which the interface characteristics are investigated [30]–[33].

Herein, a new stepwise hydrothermal growth of ZnO-NiO heteronanostructures with the contribution of Ni^{2+} ions synthesized by the hydrothermal method and increased by volume on the FTO substrate is presented. Furthermore, the surface morphology and optical properties of new ZnO-NiO heteronanostructures on the substrate were investigated for the possible development of analytical devices. The results show that heteronanostructures form between ZnO and NiO. Moreover, these heteronanostructures exhibit good performance in practical applications, indicating that they are suitable potential candidate.

II. EXPERIMENTAL

A. CHEMICALS/MATERIALS

The chemicals zinc nitrate hexahydrate ($Zn(NO_3)_2 \cdot 6H_2O$ was obtained from Alfa aesar. Nickel chloride hexahydrate ($NiCl_2 \cdot 6H_2O$), sodium hydroxide (NaOH), ethanol (C_2H_5OH), and acetone (C_3H_6O) were purchased from Merck. Deionized water (DIW) (∼18 MΩcm) was used as the solvent.

B. PREPARATION OF Ni DOPPING ZnO NANOSTRUCTURES ON FTO SUBSRATE

FTO (fluorine doped tin oxide) coated substrates were cleaned with ethanol, acetone and DIW. Subsequent, the substrates were dried at room temperature. ZnO-NiO heteroronanostructures were produced in a one-step process. The hydrothermal method [34, 35] was used to create ZnO samples and doped nickel to ZnO samples from 50 mL of solution containing 30 mM $Zn(NO_3)_2.6H_2O$, 5 mM $NiCl_2.6H_2O$, and NaOH at pH = 9.5. The concentrations of known Zn^{2+} and doped Ni^{2+} ions were made with a volumetric (v/v) relationship in the experiment, so that the total volume was 50 mL. Table 1 lists all experimental solution conditions. The hydrothermal reaction was carried out for 20 hours at 90 °C for the hydrothermal treatment. The thin films were then annealed at 450 °C on the FTO substrates. Figure 1 depicts the manufacturing process for ZnO nanostructures and ZnO-NiO heteronanostructures.

Table 1. *Includes the volumetric (v/v) values of known concentrations of Zn^{2+} and doped Ni^{2+} ions.*

Samples	30 mM Zn^{2+}	5 mM Ni^{2+}	pH
S_1	50.00 mL	---	9.50
S_2	47.50 mL	2.50 mL	9.50
S_3	45.00 mL	5.00 mL	9.50
S_4	40.00 mL	10.00 mL	9.50

C. CHARACTERIZATION

ZnO sample X-ray diffraction (XRD) patterns were acquired with a Rigaku Multiflex diffraction meter utilization CuKa radiation (λ = 1.5418 Å). The surface morphology of the produced undoped nickel to ZnO and doped nickel to ZnO samples was inspected by scanning electron microscopy (SEM) and

energy dispersive spectroscopy (EDS) analysis utilization a FEI Quanta FEG 250. The absorbance properties of nickel-free ZnO and nickel-containing ZnO heteronanostructure samples were obtained using a PG Instruments T80+ UV/VIS spectrometer.

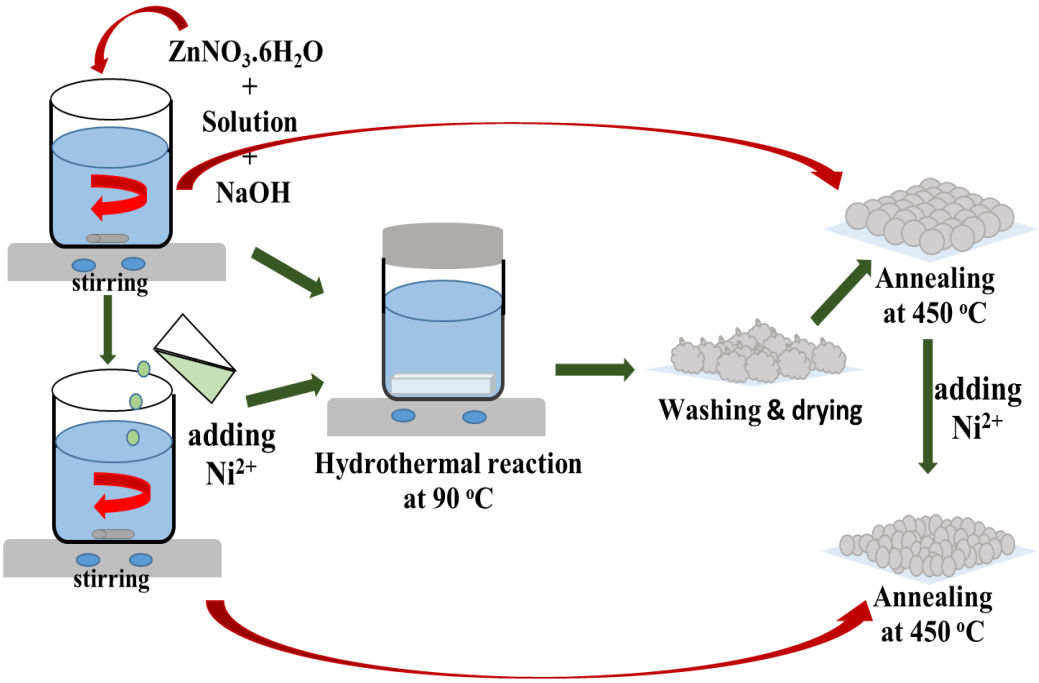

Figure 1. *Synthesis scheme of ZnO and Ni doping metal oxide heteronanostructure thin films.*

III. RESULTS AND DISCUSSION

The correspondent XRD pattern of nanostructured ZnO thin films (S_1) deposited on the FTO substrate is shown in Figure 2. When the acquired diffraction peaks are looked into, 3 peaks with high intensity are seen. It is seen that these diffraction peaks are indexed respectively (1 0 0), (0 0 2), (1 0 1). Moreover, besides these peaks, there are other diffraction peaks with low intensity. These peaks are (1 0 2), (1 1 0), (1 0 3) and (1 1 2) indexed diffraction peaks, respectively. This XRD diffraction pattern can be attributed to the crystal structures of the hexagonal phase of wurtzite nanostructured ZnO thin films (JCPDS card No: 01-089-0511). The existence of phases of the nanostructured ZnO thin film indicates the coming into being of the composite structure. XRD shape shows that nanostructured ZnO thin films with diffraction peaks are at 2θ angles. ZnO XRD is compatible with XRD models for nanostructured ZnO thin films in the literatüres [12], [36].

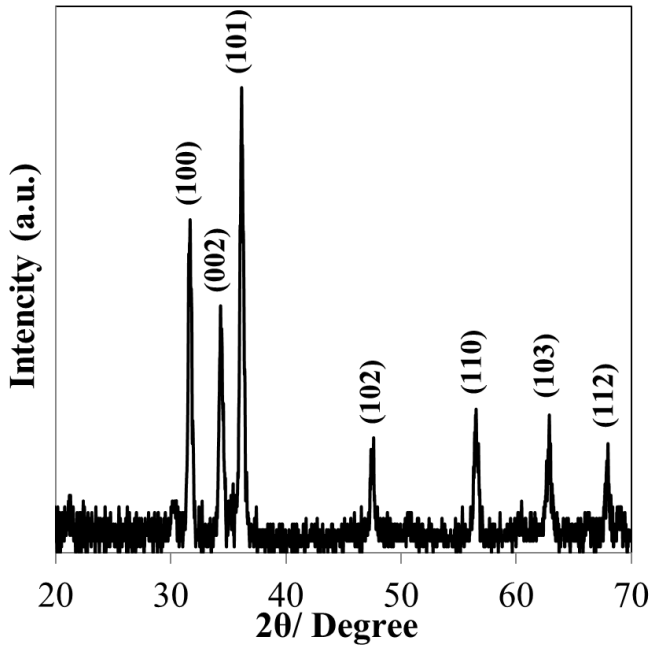

Figure 2. *XRD pattern of the ZnO nanostructure thin films deposited on FTO.*

The morphological properties of the ZnO nanostructured thin film, and the ZnO-NiO heteronanostructure thin films obtained by Ni doping at different volum Ni^{2+}/Zn^{2+} rates are shown in Figure 3. Figure 3a for S_1 shows that nanostructured ZnO thin films grow homogeneously on FTO. The surface of ZnO nanostructures is smooth and consists of four angular ZnO nanostructures in width average ~200 nm and length average ~700 nm. In the presence of 2.5 mL of Ni (5 mM) doping for S_2, it can be said that nanostructured ZnO thin films grow homogeneously and have a similar morphological structure and are arranged in a width of average approximately 150 and length 400 nm (Figure 3b). In the presence of 5 mL of Ni (5 mM) doping for S_3, the nanostructured thin films showed a homogeneous distribution, showing beautiful nanostructures with a width of about 100 and length 250 nm (Figure 3c). The morphological status of S_4 in the presence of 10 mL of Ni doping showed a homogeneous distribution with a particle size of avarege approximately 50 nm. According to S_1 sample, the particle size of Ni-doping ZnO nanostructured thin films on the FTO substrate grown with the participation of Ni for S_2, S_3, and S_4 samples appears to be reduced. As seen in the figure, the particle size is the smallest in the S4 sample with the highest Ni content. In addition, these structures show the formation of compact conformal coatings. Based on the SEM results, it is seen that the particle size decreases as increasing Ni is doped. The reason for this is that the atomic and ion radii of the element Ni are lower than the atomic and radius values of the element Zn. Moreover, it means that the Zn atom was replaced by the Ni atom and played a role in the reduction of particle size. Therefore, the role of heteronanostructure formation in the growth of ZnO nanostructure thin films by Ni doping is obvious. Thus, SEM images show the composition of homogeneously ZnO-NiO heteronanostructure thin films [37], [38].

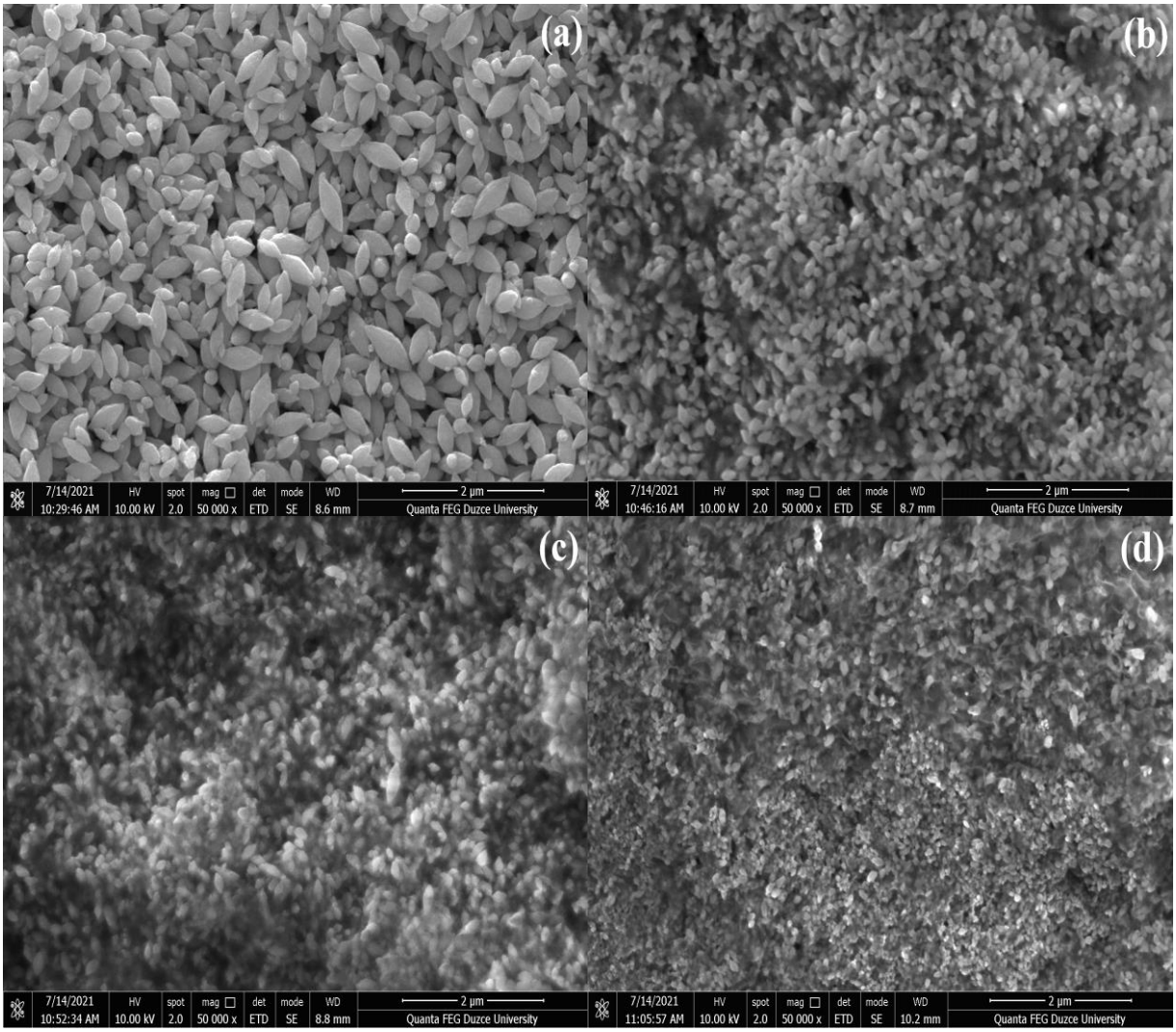

Figure 3. *SEM images of S_1* ***(a)****, S_2* ***(b)****, S_3* ***(c)*** *and S_4* ***(d)*** *various deposition on FTO substrates.*

EDS analysis was performed to identify the element ratios of ZnO nanostructure thin films and Ni-doped ZnO nanostructured thin films. The EDS spectra of the nanostructured thin films obtained for S_1 and S_4 are shown in Figure 4, respectively. For S_1, Zn and O element peaks indicate the existence of ZnO. The spectra show that the mean atomic ratio of Zn and O of ZnO nanostructure thin films is close to each other (Fig. 4a). For S_4, there are Zn, Ni and O element peaks. When we look at the spectra here, it shows that the Zn element has been replaced by the Ni element in % atomic ratio (Figure 4b). This means that heteronanostructure thin films are formed, and the atomic % ratios formed support this situation when the results obtained with SEM images are examined. In addition, % atomic EDS analysis spectrum ratios obtained for S_1-S_4 samples are given in Table-2, respectively. When Table-2 is examined, it is seen that as Ni is added to the environment, the amount of Ni increases in atomic % ratios, the amount of Zn decreases and the amount of O does not change significantly. EDS analysis results of metal doping metal oxide nanostructured thin films were similar to ZnO-NiO heteronanostructures in the literature [39].

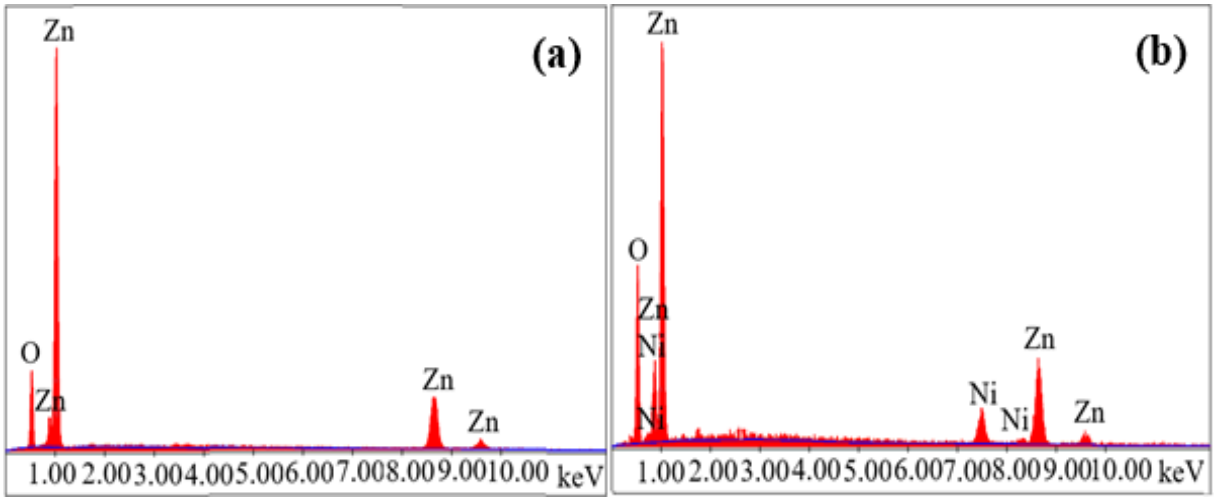

Figure 4. *EDS patterns of the ZnO nanostructure thin films and ZnO-NiO heteronanostructure thin films deposited with* ***(a)*** *S1 and* ***(b)*** *S4.*

Table 2. *% atomic values of Zn, Ni and O from EDS analysis results of S_1-S_4 samples.*

Samples	Zn % At.	Ni % At.	O % At.
S_1	48.80	---	51.20
S_2	45.56	3.42	51.02
S_3	42.12	5.21	52.67
S_4	38.02	8.68	53.30

The optical properties of ZnO thin films in the absence and presence of Ni deposited for 20 h were investigated by the UV-vis absorption spectrum measured in the wavelength range of 300-800 nm (Fig. 5). The film shows good absorption in the visible region and the ultraviolet region. From the absorbance data, the absorption coefficient α was calculated using Lambert's law [40].

$$2.303A = \alpha d \quad (1)$$

where A is the optical absorbance and d is the film thickness. On the other hand, the optical band gap of the thin film was determined by applying the Tauc relationship given by:

$$\alpha h\nu = A_o[h\nu - E_g]^n \quad (2)$$

where hν is the photon energy, E_g is the band gap energy and A_o is a constant which is related to the effective masses associated with the bands [41]. UV-vis absorbance spectroscopy was performed to obtain the influence on the optical properties of nanostructured ZnO thin films deposited on FTO substrates and nanostructured ZnO-NiO thin films formed by doping with increasing Ni content. The band gap values of the resulting nanostructured thin films were calculated by making a sign $(\alpha h\nu)^2$ against hν and subtracting the linear part of the graph to the energy pivot (Fig. 5a–d). The absorption characeristics of thin films is related to the energy bands of both ZnO nanostructure thin films and ZnO-NiO nanostructure thin films with S_1, S_2, S_3 and S_4 structures, respectively. The optical absorption

spectrum analysis of ZnO nanostructured films is more intense and wider in the visible light zone. However, the absorption spectrum of thin films doped with increasing Ni content is seen to pass into the ultraviolet region. From the optical spectrum figures, a modification in wavelength of Ni-doping metal oxide nanostructure films (S_2-S_4) is observed comparison to S_1. Here, it was shown that nanostructured ZnO thin films formed crystals according to the increasing Ni content and interacted with ZnO in the deposition process. Moreover, this interaction constitutes the formation of nanostructured ZnO-NiO thin films. This is an indication of the formation of ZnO-NiO heteronanostructure. Thus, a leftward change in wavelengths is noticed with increasing Ni amount. The value of n is equal to 1/2 for a direct band gap material and 2 for indirect gap. The absorption ($\alpha \geq 10^4$ cm^{-1}) is related to direct band transitions [42]. The absorption coefficient for the film supporting the direct band gap property of the metal oxide semiconductor was found above the value. Based on these UV-vis optical absorption informations, the optical spectrum band gaps of both nanostructured ZnO thin films and ZnO-NiO heteronanostructure thin films were calculated from extrapolating of the linear part of $(\alpha h\nu)^2$ against the hν plot at $\alpha = 0$. The results were 2.94 eV, 3.23 eV, 3.32 eV and 3.38 eV, respectively. These results are in good procedure with beforehand reported values for both ZnO thin films and ZnO-NiO thin films [43], [44].

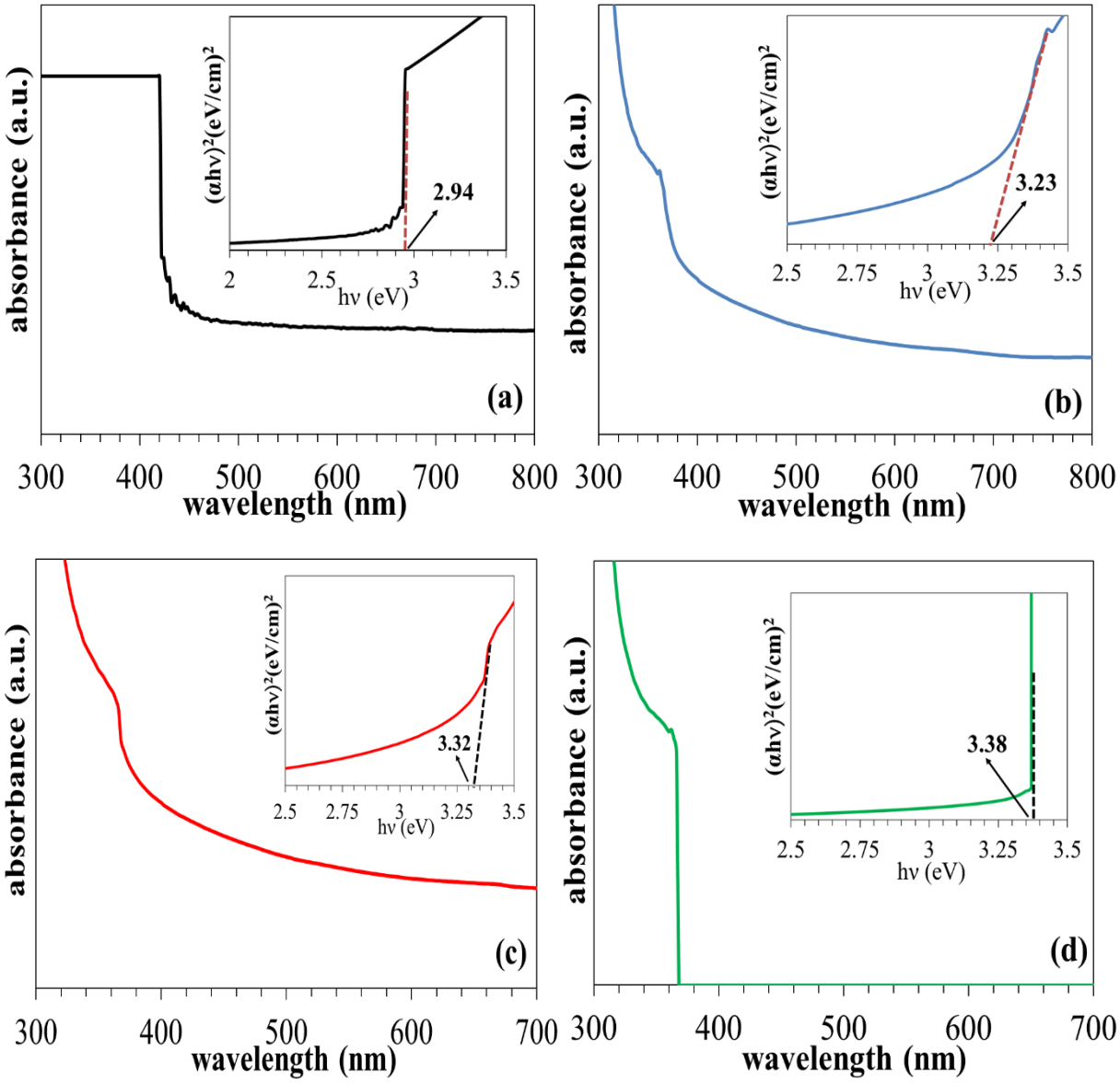

Figure 5. *Absorption spectrums and band gap values of the ZnO nanostructures and ZnO-NiO nanostructure thin films deposited with (a) S_1, (b) S_2, (c) S_3 and (d) S_4.*

IV. CONCLUSIONS

ZnO thin films and ZnO-NiO heterostructure thin films were depozited on FTO coated glasses at pH = 9.5 conditions, and their morphological and optical properties were investigated. It was observed that ZnO nanostructures and Ni doping-ZnO nanostructures on FTO grew homogeneously and their surfaces were smooth. Morphological studies increased the Ni content of the films from 0 to 10 mL, and it was determined that the particle sizes of the nanostructures decreased with increasing Ni content. This can be expressed as evidence that a heteronano structure is formed between p-type NiO and n-type ZnO according to the increasing Ni content. Optical absorption studies showed that the absorption spectrum of ZnO nanostructured films was determined to pass from the visible light region to the ultraviolet region of the absorption spectrum of heteronanostructure thin films doped with increasing Ni content. In this case, it supports the formation of a structure between ZnO and NiO nanostructures. The results show that the ZnO-NiO heteronano structure has good performance for practical applications and is a potential candidate for further studies such as solar cells, sensors and light-emitting diodes.

ACKNOWLEDGEMENTS: This study was supported by Düzce University Scientific Research Projects (Proje no: 2021.05.03.1250).

V. REFERENCES

[1] U. T. Nakate et al., "Improved selectivity and low concentration hydrogen gas sensor application of Pd sensitized heterojunction n-ZnO/p-NiO nanostructures," J. Alloys Compd., vol. 797, pp. 456–464, 2019, doi: 10.1016/j.jallcom.2019.05.111.

[2] S.K. Tripathi, R. Kaur, M. Rani "Oxide Nanomaterials and their Applications as a Memristor," Solid State Phenomena, vol. 222, pp. 67-97, 2015, doi:10.4028/www.scientific.net/SSP.222.67.

[3] K. Al-Mayalee, N. S. Saadi, E. Badradeen, F. Watanabe, and T. Karabacak, "Optical and Photoconductive Response of CuO Nanostructures Grown by a Simple Hot-Water Treatment Method," J. Phys. Chem. C, 122, 41, 23312–23320, 2018, doi: 10.1021/acs.jpcc.8b06783.

[4] G. Neumark, Y. Gong, and I. Kuskovsky, "Doping Aspects of Zn-Based Wide-Band-Gap Semiconductors," Springer Handbooks, vol. 3, pp. 843–854, 2007, doi: 10.1007/978-0-387-29185-7_35.

[5] Z. Fan and J. G. Lu, "Zinc oxide nanostructures: Synthesis and properties," J. Nanosci. Nanotechnol., vol. 5, no. 10, pp. 1561–1573, 2005, doi: 10.1166/jnn.2005.182.

[6] A. Janotti and C. G. Van De Walle, "Fundamentals of zinc oxide as a semiconductor," Reports Prog. Phys., vol. 72, no. 12, 2009, doi: 10.1088/0034-4885/72/12/126501.

[7] Y. Zhang, M. K. Ram, E. K. Stefanakos, and D. Y. Goswami, "Synthesis, characterization, and applications of ZnO nanowires," J. Nanomater., vol. 2012, 2012, doi: 10.1155/2012/624520.

[8] J. S. Wellings, N. B. Chaure, S. N. Heavens, and I. M. Dharmadasa, "Growth and characterisation of electrodeposited ZnO thin films," Thin Solid Films, vol. 516, no. 12, pp. 3893–3898, 2008, doi: 10.1016/j.tsf.2007.07.156.

[9] Z. Lin and J. Song, “Piezoelectric Nanogenerators Based on Zinc Oxide Nanowire Arrays Author(s): Zhong Lin Wang and Jinhui Song Source:,” Science (80-.)., vol. 312, no. 5771, pp. 242–246, 2006, doi: 10.1126/science.1124005.

[10] L. Vayssieres, K. Keis, A. Hagfeldt, and S. E. Lindquist, “Three-dimensional array of highly oriented crystalline ZnO microtubes,” Chem. Mater., vol. 13, no. 12, pp. 4395–4398, 2001, doi: 10.1021/cm011160s.

[11] A. Wibowo et al., “ZnO nanostructured materials for emerging solar cell applications,” RSC Adv., vol. 10, no. 70, pp. 42838–42859, 2020, doi: 10.1039/d0ra07689a.

[12] M. Biçer, M. Gökçen, and E. Orhan, “Fabrication and Photoanode Performance of ZnO Nanoflowers in ZnO-Based Dye-Sensitized Solar Cells,” SSRN Electron. J., vol. 131, no. June, pp. 2–7, 2022, doi: 10.2139/ssrn.4072317.

[13] N. Izu et al., “Polyol synthesis of Al-doped ZnO spherical nanoparticles and their UV-vis-NIR absorption properties,” Ceram. Int., vol. 40, no. 6, pp. 8775–8781, 2014, doi: 10.1016/j.ceramint.2014.01.099.

[14] M. Rajalakshmi, S. Sohila, S. Ramya, R. Divakar, C. Ghosh, and S. Kalavathi, “Blue green and UV emitting ZnO nanoparticles synthesized through a non-aqueous route,” Opt. Mater. (Amst)., vol. 34, no. 8, pp. 1241–1245, 2012, doi: 10.1016/j.optmat.2012.01.021.

[15] C. A. Jaramillo-Páez, J. A. Navío, M. C. Hidalgo, and M. Macías, “ZnO and Pt-ZnO photocatalysts: Characterization and photocatalytic activity assessing by means of three substrates,” Catal. Today, vol. 313, no. December 2017, pp. 12–19, 2018, doi: 10.1016/j.cattod.2017.12.009.

[16] X. Chen, Z. Wu, D. Liu, and Z. Gao, “Preparation of ZnO Photocatalyst for the Efficient and Rapid Photocatalytic Degradation of Azo Dyes,” Nanoscale Res. Lett., vol. 12, no. 1, pp. 4–13, 2017, doi: 10.1186/s11671-017-1904-4.

[17] J. Xie, Y. Cao, D. Jia, Y. Li, and Y. Wang, “Solid-state synthesis of Y-doped ZnO nanoparticles with selective-detection gas-sensing performance,” Ceram. Int., vol. 42, no. 1, pp. 90–96, 2016, doi: 10.1016/j.ceramint.2015.07.135.

[18] J. Guo and C. Peng, “Synthesis of ZnO nanoparticles with a novel combustion method and their C2H5OH gas sensing properties,” Ceram. Int., vol. 41, no. 2, pp. 2180–2186, 2015, doi: 10.1016/j.ceramint.2014.10.017.

[19] M. C. Li et al., “Effect of annealing temperature on the optoelectronic properties and structure of NiO films,” Ceram. Int., vol. 48, no. 2, pp. 2820–2825, 2022, doi: 10.1016/j.ceramint.2021.10.071.

[20] G. T. Anand, R. Nithiyavathi, R. Ramesh, S. John Sundaram, and K. Kaviyarasu, “Structural and optical properties of nickel oxide nanoparticles: Investigation of antimicrobial applications,” Surfaces and Interfaces, vol. 18, no. February, p. 100460, 2020, doi: 10.1016/j.surfin.2020.100460.

[21] P. Iyyappa Rajan et al., “Green-fuel-mediated synthesis of self-assembled NiO nano-sticks for dual applications-photocatalytic activity on Rose Bengal dye and antimicrobial action on bacterial strains,” Mater. Res. Express, vol. 4, no. 8, 2017, doi: 10.1088/2053-1591/aa7e3c.

[22] A. A. Ezhilarasi, J. J. Vijaya, L. J. Kennedy, and K. Kaviyarasu, “Green mediated NiO nano-rods using Phoenix dactylifera (Dates) extract for biomedical and environmental applications,” Mater. Chem. Phys., vol. 241, no. November 2019, p. 122419, 2020, doi: 10.1016/j.matchemphys.2019.122419.

[23] S. T. Fardood, A. Ramazani, and S. Moradi, “A novel green synthesis of nickel oxide nanoparticles using arabic gum,” Chem. J. Mold., vol. 12, no. 1, pp. 115–118, 2017, doi: 10.19261/cjm.2017.383.

[24] A. A. Ezhilarasi, J. J. Vijaya, K. Kaviyarasu, M. Maaza, A. Ayeshamariam, and L. J. Kennedy, “Green synthesis of NiO nanoparticles using Moringa oleifera extract and their biomedical applications: Cytotoxicity effect of nanoparticles against HT-29 cancer cells,” J. Photochem. Photobiol. B Biol., vol. 164, pp. 352–360, 2016, doi: 10.1016/j.jphotobiol.2016.10.003.

[25] M. El-Kemary, N. Nagy, and I. El-Mehasseb, “Nickel oxide nanoparticles: Synthesis and spectral studies of interactions with glucose,” Mater. Sci. Semicond. Process., vol. 16, no. 6, pp. 1747–1752, 2013, doi: 10.1016/j.mssp.2013.05.018.

[26] M. A. Ciolan and I. Motrescu, “Pulsed Laser Ablation: A Facile and Low-Temperature Fabrication of Highly Oriented n-Type Zinc Oxide Thin Films,” Appl. Sci., vol. 12, no. 2, 2022, doi: 10.3390/app12020917.

[27] T. P. Mokoena et al., “Enhanced propanol gas sensing performance of p-type NiO gas sensor induced by exceptionally large surface area and crystallinity,” Appl. Surf. Sci., vol. 571, no. April 2021, p. 151121, 2022, doi: 10.1016/j.apsusc.2021.151121.

[28] L. Zhu, Y. Li, and W. Zeng, “Hydrothermal synthesis of hierarchical flower-like ZnO nanostructure and its enhanced ethanol gas-sensing properties,” Appl. Surf. Sci., vol. 427, no. 3, pp. 281–287, 2018, doi: 10.1016/j.apsusc.2017.08.229.

[29] N. D. Hoa, P. Van Tong, C. M. Hung, N. Van Duy, and N. Van Hieu, “Urea mediated synthesis of Ni(OH)2 nanowires and their conversion into NiO nanostructure for hydrogen gas-sensing application,” Int. J. Hydrogen Energy, vol. 43, no. 19, pp. 9446–9453, 2018, doi: 10.1016/j.ijhydene.2018.03.166.

[30] P. Dai, T. tao Yan, X. xin Yu, Z. man Bai, and M. zai Wu, “Two-Solvent Method Synthesis of NiO/ZnO Nanoparticles Embedded in Mesoporous SBA-15: Photocatalytic Properties Study,” Nanoscale Res. Lett., vol. 11, no. 1, 2016, doi: 10.1186/s11671-016-1445-2.

[31] J. Cai, R. Li, J. Cao, J. Liu, J. Han, and M. Huang, “Plasmonic Au-decorated hierarchical p-NiO/n-ZnO heterostructure arrays for enhanced photoelectrochemical water splitting,” Phys. E Low-Dimensional Syst. Nanostructures, vol. 135, no. September 2021, p. 114974, 2022, doi: 10.1016/j.physe.2021.114974.

[32] P. Sahoo, A. Sharma, S. Padhan, and R. Thangavel, “Construction of ZnO@NiO heterostructure photoelectrodes for improved photoelectrochemical performance,” Int. J. Hydrogen Energy, vol. 46, no. 73, pp. 36176–36188, 2021, doi: 10.1016/j.ijhydene.2021.08.154.

[33] C. Su et al., “Glucose-assisted synthesis of hierarchical NiO-ZnO heterostructure with enhanced glycol gas sensing performance,” Sensors Actuators, B Chem., vol. 329, no. March 2020, p. 129167, 2021, doi: 10.1016/j.snb.2020.129167.

[34] M. Biçer, “One-Step Hydrothermal Deposition of ZnO–TiO_2 Heterojunction Nanostructures as Photoelectrochemical Performance for Sb_2S_3 Quantum-Dot-Sensitized Solar Cells by High-Efficiency Enhancement,” Crystallogr. Reports, vol. 66, no. 6, pp. 1117–1124, 2021, doi: 10.1134/S1063774521060067.

[35] M. Biçer, “ZnO-TiO_2 Hetero Nanoyapılarının Sentezi ve Güneş Pilleri için Fotoelektrokimyasal Performansı” Düzce Üniversitesi Bilim ve Teknol. Derg., vol. 9, 262–272, 2021, doi: 10.29130/dubited.840584.

[36] M. A. Shafi, A. Bouich, K. Fradi, J. M. Guaita, L. Khan, and B. Mari, “Effect of deposition cycles on the properties of ZnO thin films deposited by spin coating method for CZTS-based solar cells,” Optik (Stuttg)., vol. 258, no. September 2021, p. 168854, 2022, doi: 10.1016/j.ijleo.2022.168854.

[37] P. K. Sharma, R. K. Dutta, and A. C. Pandey, “Effect of nickel doping concentration on structural and magnetic properties of ultrafine diluted magnetic semiconductor ZnO nanoparticles,” J. Magn. Magn. Mater., vol. 321, no. 20, pp. 3457–3461, 2009, doi: 10.1016/j.jmmm.2009.06.055.

[38] G. Vijayaprasath et al., “Role of nickel doping on structural, optical, magnetic properties and antibacterial activity of ZnO nanoparticles,” Mater. Res. Bull., vol. 76, pp. 48–61, 2016, doi: 10.1016/j.materresbull.2015.11.053.

[39] Y. Liu, G. Li, R. Mi, C. Deng, and P. Gao, “An environment-benign method for the synthesis of p-NiO/n-ZnO heterostructure with excellent performance for gas sensing and photocatalysis,” Sensors Actuators, B Chem., vol. 191, pp. 537–544, 2014, doi: 10.1016/j.snb.2013.10.068.

[40] A. Adachi, A. Kudo, T. Sakata, “The Optical and Photoelectrochemical Properties of Electrodeposited CdS and SnS Thin Films,” Bull. Chem. Soc. Jpn, vol. 68, pp. 3283-3288, 1995, doi: 10.1246/bcsj.68.3283.

[41] M. Biçer, İ. Şişman, “Electrodeposition and growth mechanism of SnSe thin films,” Appl. Surf. Sci, vol. 257, pp. 2944–2949, 2011, doi:10.1016/j.apsusc.2010.10.096.

[42] K. R. Rajesh, C. S. Menon, “Electrical and optical properties of vacuum deposited MnPc thin films,” Eur. Phys. J. B, vol. 47, pp. 171, 2005, doi: 10.1140/epjb/e2005-00317-x.

[43] G. Srinet, R. Kumar, and V. Sajal, “Structural, optical, vibrational, and magnetic properties of sol-gel derived Ni doped ZnO nanoparticles,” J. Appl. Phys., vol. 114, no. 3, 2013, doi: 10.1063/1.4813868.

[44] R. N. Ali, H. Naz, J. Li, X. Zhu, P. Liu, and B. Xiang, “Band gap engineering of transition metal (Ni/Co) codoped in zinc oxide (ZnO) nanoparticles,” J. Alloys Compd., vol. 744, pp. 90–95, 2018, doi: 10.1016/j.jallcom.2018.02.072.